Radiative Topological States in Resonant Photonic Crystals

A. V. Poshakinskiy,[1,*] A. N. Poddubny,[1] L. Pilozzi,[2] and E. L. Ivchenko[1]

[1]*Ioffe Physical-Technical Institute of the Russian Academy of Sciences, 194021 St. Petersburg, Russia*
[2]*Istituto dei Sistemi Complessi, CNR, C. P. 10, Monterotondo Stazione, Rome I-00016, Italy*

We present a theory of topological edge states in one-dimensional resonant photonic crystals with a compound unit cell. Contrary to the conventional electronic topological states, the modes under consideration are radiative; i.e., they decay in time due to the light escape through the structure boundaries. We demonstrate that the edge states survive despite their radiative decay and can be detected both in time- and frequency-dependent light reflection.

Introduction.—A topological insulator is an electronic material that has a band gap in its interior like an ordinary insulator but possesses conducting states on its edge or surface. The surface states of topological insulators have been extensively studied both in two-dimensional (2D) and three-dimensional (3D) materials [1]. Recently an untrivial link has been revealed between such seemingly distinct systems as topological insulators, one-dimensional (1D) quasicrystals, and periodic 1D crystals with compound unit cell [2–5] (see also the viewpoint Ref. [6]). In particular, it has been demonstrated that the 1D Aubry-André-Harper (AAH) model, or a "bichromatic" system (both incommensurate and commensurate), exhibits topological properties similar to those attributed to systems of a higher dimension [2,3]. This model allows states at boundaries between two distinct topological systems. The system is described by a 1D tight-binding Hamiltonian with nearest-neighbor hopping and an on-site potential. In the generalized AAH model both the hopping terms and on-site potential are cosine modulated [5]. It is the modulation phase that adds the second degree of freedom and permits one to relate the descendent 1D model with a 2D "ancestor" system that has a 2D band structure and quantized Chern numbers. In this Letter, instead of quasiparticles that tunnel from one site to another, we consider a 1D sequence of sites with resonant excitations long-range coupled through an electromagnetic field [7]. Such a system is open, its eigenfrequencies are complex, and its eigenstates are quasistationary due to the radiative decay. Hence, the resonant optical lattice stands out of the standard classification of topological insulators, developed for conservative and Hermitian electronic problems [8]. We show here that this 1D bichromatic resonant photonic crystal demonstrates the topological properties in spite of being open and formulate general conditions for the edge state existence. We also demonstrate how the radiative character of the system opens new pathways to optical detection of the edge states. This provides an important insight into the rapidly expanding field of the

electromagnetic topological states in photonic crystals [9,10], coupled cavities [11,12], waveguide arrays [13–15], metamaterials [16], and plasmonic chains [17].

Model.—We consider a 1D resonant photonic crystal consisting of alternating layers $\mathcal{A}$ and $\mathcal{B}$. The dielectric constant ε_b of the material $\mathcal{B}$ is frequency-independent while the thin layer $\mathcal{A}$ is characterized by single-pole amplitude coefficients of light reflection and transmission,

$$r_\mathcal{A}(\omega) = -\frac{i\Gamma_0}{\omega - \omega_0 + i(\Gamma_0 + \Gamma)},$$
$$t_\mathcal{A}(\omega) = 1 + r_\mathcal{A}(\omega). \tag{1}$$

Here, ω is the light frequency, the resonance frequency ω_0, radiative (Γ_0) and nonradiative (Γ) decay rates are three basic parameters of the excitation in a single layer $\mathcal{A}$ sandwiched between semi-infinite layers $\mathcal{B}$. The model can be applied to excitonic [18], dielectric and plasmonic multilayers [19,20], coupled waveguides [21], and even to nuclear excitations in multilayers containing different isotopes of the same element, see the review [7]. The multilayer system can be equivalently described by a set of coupled equations for the resonant dielectric polarizations P_n of the layers $\mathcal{A}$ ($n = 1, 2....$), as follows

$$(\omega_0 - \omega)P_n - i\Gamma_0 \sum_{n'} \Lambda_{nn'} P_{n'} = 0, \tag{2}$$

where $\Lambda_{nn'} = e^{iq|z_n - z_{n'}|}$, $q = \omega\sqrt{\varepsilon_b}/c$ is the light wave vector in the material $\mathcal{B}$ and z_n is the center of the nth layer $\mathcal{A}$ [18]. Following Ref. [4] we take a bichromatic structure with the $\mathcal{A}$ layers centered at

$$z_n = d[n + \eta\cos(2\pi bn + \phi)], \tag{3}$$

where b is a dimensionless parameter of the system, d is the period in the primary lattice, and η is a small modulation amplitude. Figure 1 illustrates the structure with $b = 1/3$
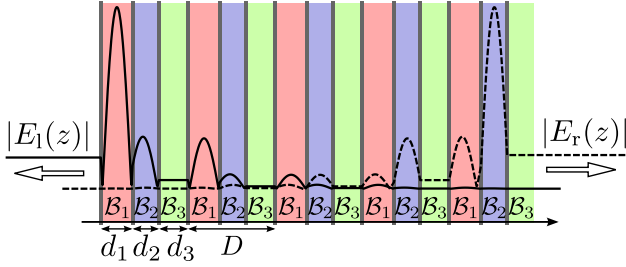
FIG. 1 (color online). Illustration of the periodic structure with three layers $\mathcal{A}$ in the unit cell. Vertical lines indicate the $\mathcal{A}$ layers, the labels $\mathcal{B}_1$, $\mathcal{B}_2$, and $\mathcal{B}_3$ mark the barriers of different thicknesses, and $d_l = z_{l+1} - z_l$ where $l = 1, 2, 3$ and $z_4 = z_1 + D$. The solid line shows the electric field distribution for the state localized on the left edge, the dashed line corresponds to the right-edge state. The parameters used are $d = \lambda_0/2$ ($\lambda_0 = 2\pi c/\sqrt{\varepsilon_b}\omega_0$), $\varkappa = \phi - \pi/6 = \pi/2$, and $\eta = 0.2/\pi$.

representing a periodic photonic crystal with the period $D = 3d$.

Topological properties of the lattice.—Let us relate the 1D multilayer system with a 2D "ancestor" lattice with the sites at $z = z_n$ and $x = m$ ($m = 0, \pm 1 \dots$), where x is an extra axis. To introduce the site polarization P_{nm} of the 2D lattice, we replace P_n by $P_{n,\phi}$ in Eq. (2), consider ϕ as the wave vector component along the x direction, and define P_{nm} by $P_{n,\phi} = \sum_{m'} e^{-im'\phi} P_{n,m'}$. After multiplying Eq. (2) by $e^{im\phi}/2\pi$ and integrating over ϕ from 0 to 2π, we obtain a 2D counterpart of Eq. (2) where $\Lambda_{nn'}$ is replaced by

$$\Lambda_{nm;n'm'} = e^{iqd|n-n'|}e^{i\pi b(m'-m)(n+n')}$$
$$\times J_{m-m'}[2\eta qd \sin(\pi b|n-n'|)], \qquad (4)$$

and J_l is the Bessel function of the order l. These coefficients retain the long-range coupling distinct from the nearest-neighbor AAH model [4]. The phases that are gained along a closed path in the clockwise and counterclockwise directions are different. This corresponds to the broken time inversion symmetry in the 2D "ancestor" system and can be interpreted as a presence of an effective magnetic field with the flux per unit cell equal to $2\pi b$. In the following we set b to be a rational number $\mathcal{M}/\mathcal{N}$ in which case the structure is periodic with the period $D = \mathcal{N}d$ and contains $\mathcal{N}$ layers $\mathcal{A}$ in the unit cell. The structure with irrational b can be smoothly transformed to that with close rational b conserving the edge state in the given bulk excitation gap [22]. The impact of the fractal band structure of resonant photonic quasicrystals [23] on the topological properties is yet to be uncovered.

The topological features of the model are revealed by the nontrivial Chern numbers of allowed zones of the infinite structure. The propagating solutions satisfy the Bloch condition $P_{l+s\mathcal{N}}(k,\phi) = e^{iskD}P_l(k,\phi)$, where the index $l = 1, 2 \dots \mathcal{N}$ enumerates the layers $\mathcal{A}$ in the unit cell, $s = 0, \pm 1 \dots$ and k is the wave vector z component defined

in the interval between $-\pi/D$ and π/D. The polarizations $P_l(k,\phi)$ satisfy the equations $\sum_{l'} H_{ll'}P_{l'} = \hbar(\Omega - \omega_0)P_l$, where the Hermitian matrix,

$$H_{ll'} = \hbar\Gamma_0 \frac{e^{-ikD\text{sign}\{l-l'\}} \sin qz_{ll'} + \sin q(D - z_{ll'})}{\cos kD - \cos qD},$$

plays the role of the Hamiltonian ($z_{ll'} = |z_l - z_{l'}|$). Due to the time-inversion symmetry, the eigenfrequency $\Omega(k,\phi)$ is an even function of k. It is convenient to make a phase shift in Eq. (3) replacing ϕ by $\varkappa - b\pi + \pi/2$ and defining the "wave vector" $\varkappa$ in the interval $(-\pi,\pi]$. The shift allows us to disclose an important symmetry property of the system: the structure corresponding to a particular value of $\varkappa$ is spatially inverted under the reversal $\varkappa \rightarrow -\varkappa$. This means that the eigenfrequency $\Omega(k,\varkappa)$ is also even in $\varkappa$. Another property $\Omega(k,\varkappa+2\pi bp) = \Omega(k,\varkappa)$ follows from the invariance of the infinite system under the shift $n \rightarrow n + p$ in Eq. (3).

The Chern number C_ν of the band ν with eigensolutions $P_l(k,\varkappa)$ is defined in a standard way as $\int_{-\pi}^{\pi} d\varkappa \int_{-\pi/D}^{\pi/D} dk(\partial_k A_\varkappa - \partial_\varkappa A_k)/(2\pi i)$, where $A_k \equiv \sum_l P_l^* \partial_k P_l$, and $A_\varkappa$ is defined similarly. As shown below, the structure must lack an inversion center in order to have nontrivial Chern numbers and topological edge states. In case of two layers $\mathcal{A}$ per unit cell one can choose the unit cell in such a way that its center is in the middle between these two layers. Such a unit cell possesses an inversion center. Thus, we need at least three layers $\mathcal{A}$ in the unit cell. Figure 2(a) presents the dependence of the edges of allowed bands on the wave vector $\varkappa$ for the lattice with $b = 1/3$, $D = 3d$ and the primary period satisfying the resonant Bragg condition $d = \lambda_0/2$ [7]. The corresponding Chern numbers are equal to -1, 2, and -1. The parameter $\varkappa$ when adiabatically varied leads to the Thouless pump of the states [4,24]. Thus, the Chern number of the band coincides with the number of left-edge states that enter the corresponding band when $\varkappa$ changes from $-\pi$ to π minus the number of those that leave the band. Real parts of the eigenfrequencies of the left- and right-edge states of the structure are depicted by solid and dashed lines in Fig. 2(a). Next we give the details of how these states are found.

Radiative edge states.—Direct calculation of the eigenfrequencies ω from Eq. (2) is a numerically challenging problem of solution of a transcendent equation with ω present in the phase factors $e^{iqd|z_n-z_{n'}|}$ through $q = \omega\sqrt{\varepsilon_b}/c$. Instead, we study properties of the structure reflection coefficient $r(\omega)$ as a function analytically continued onto the complex plane. As an additional advantage, the coefficient $r(\omega)$ can be readily evaluated using the transfer matrix technique [18] and is directly accessible in experiments on photonic crystals. It is instructive to start from the analytical properties of the reflection coefficient $r_\infty(\omega)$ from the semi-infinite structure. This function of ω has poles indicating the edge states and discontinuities
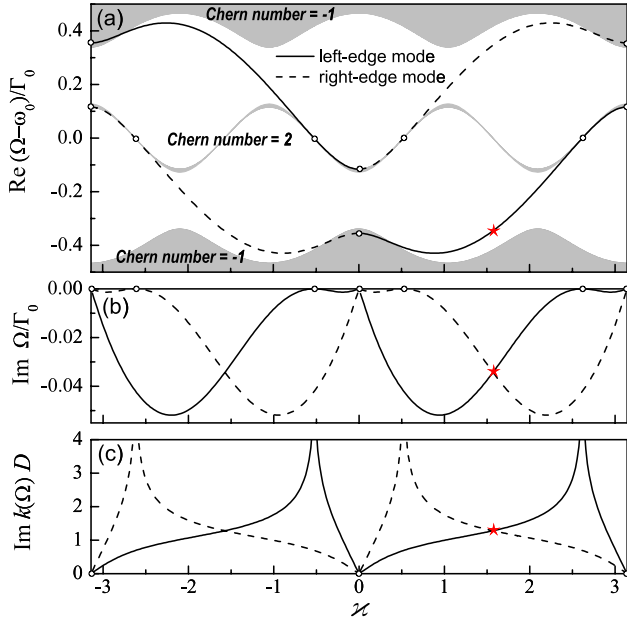
FIG. 2 (color online). (a) The band structure as a function of the "ancestor" lattice wave vector $\varkappa = \phi - \pi/6$ characterizing the distribution of three $\mathcal{A}$ layers in the unit cell. The gray regions are the allowed polariton zones, while the white regions are the stop bands. The lines show the dependence of the real part of the frequency of the left-edge (solid) and the right-edge (dashed) mode. Circles indicate points where the edge modes are absent. The star shows the value of $\varkappa = \pi/2$ used in Fig. 3. (b) Dependence of the edge mode decay rate ImΩ on the parameter $\varkappa$. (c) The $\varkappa$ dependence of the eigenstate spatial decay constant Im$\{k(\Omega)\}D$. The calculation is performed for $d = \lambda_0/2$, $b = 1/3$, $\eta = 0.2/\pi$, and $\Gamma = 0$.

across the branch cuts on the real axis related to allowed bands of the corresponding infinite structure. In the reflection coefficient from the finite structure the cuts are replaced by poles due to the Fabry-Pérot interference. In thick structures the poles of $r(\omega)$ related to the edge states are close to those of $r_\infty(\omega)$ and, therefore, can be easily distinguished.

We characterize each structure layer by a 2×2 transfer matrix linking the amplitudes of the right- and left-going waves (denoted by $+$ and $-$, respectively) at the right layer edge with those at the left one. For a single layer $j = \mathcal{A}, \mathcal{B}$, this matrix reads

$$\hat{T}^{(j)}(\omega) = \frac{1}{t_j(\omega)} \begin{bmatrix} t_j^2(\omega) - r_j^2(\omega) & r_j(\omega) \\ -r_j(\omega) & 1 \end{bmatrix}, \quad (5)$$

where the single layer reflection and transmission coefficients r_j, t_j are given by Eq. (1) for a resonant layer $\mathcal{A}$ while, for a spacing layer $\mathcal{B}$ of the width L, they are $r_\mathcal{B} = 0$, $t_\mathcal{B} = e^{iqL}$. The total transfer matrix of the structure $\hat{T}^{(N)}(\omega)$ is a product of individual transfer matrices through N periods. The reflection coefficient from the left reads [18] $r_N(\omega) = -T_{-+}^{(N)}(\omega)/T_{--}^{(N)}(\omega)$. As follows from Eqs. (1) and

(5) the transfer matrix elements for a single layer have no poles except for the trivial pole $\omega_0 - i\Gamma$. Hence, the pole Ω of $r_N(\omega)$ can be found from the condition $T_{--}^{(N)}(\Omega) = 0$. This condition allows the existence of light waves going away from the system in the absence of incident waves, and thus it indeed determines the eigenmodes. For real ω the reflectance and transmittance are bounded by unity. Therefore, all the pole frequencies Ω should have nonzero imaginary parts and the corresponding eigenstates decay in time.

The similar consideration can be applied to a semi-infinite structure. Its reflection coefficient is expressed in terms of the transfer matrix through one period as

$$r_\infty(\omega) = \frac{e^{ik(\omega)D} - T_{++}^{(1)}(\omega)}{T_{+-}^{(1)}(\omega)}, \quad (6)$$

where $e^{ik(\omega)D}$ is an eigenvalue of the matrix $\hat{T}^{(1)}(\omega)$ and the polariton wave vector $k(\omega)$ is chosen to have positive Im$k(\omega)$. The poles of $r_\infty(\omega)$ are found from

$$T_{+-}^{(1)}(\Omega) = 0, \qquad |T_{--}^{(1)}(\Omega)| < 1. \quad (7)$$

The first condition means that only the outgoing wave is present on the left side of the structure, while the second condition ensures the eigenstate to decay spatially inside the structure. Hence, the conditions (7) select modes attached to the left edge. To find the right-edge modes one should replace the first condition with $T_{-+}^{(1)}(\Omega) = 0$.

Results and discussion.—First we briefly consider a structure with $b = 1/2$ and two resonant layers in the period. Its unit cell can be chosen to have a center of symmetry. In this case $T_{+-}^{(1)} = -T_{-+}^{(1)}$ (see e.g. Ref. [25]); at the frequency of a possible pole of r_∞, the off-diagonal elements of matrices $\hat{T}^{(1)}$ and $\hat{T}^{(N)} = \hat{T}^{(1)N}$ are zeros, and the reflection coefficient $r_N = -T_{-+}^{(N)}/T_{--}^{(N)}$ vanishes rather than having a pole and, thus, the edge states are absent. Concomitantly, in the structure with $b = 1/2$ the eigensolutions $P_l(k, \varkappa)$ of the Hamiltonian $H_{ll'}$ can be chosen as satisfying $P_l(k, \varkappa) = P_l(k, -\varkappa)$. As a result, the Berry curvature is odd in $\varkappa$ and all the Chern numbers are zero. The absence of radiative edge states is characteristic for centrosymmetric optical lattices. The conventional electronic lattices may have edge (zero-energy) modes even for a centrosymmetric unit cell, e.g., in the Su-Schrieffer-Heeger model with two sites per unit cell [24].

Now we turn to the lattice with $b = 1/3$ comprising three resonant layers per period. The dependence of the spectrum on the auxiliary wave vector component $\varkappa$ is presented in Fig. 2. We fix the attention on the narrow spectral range around the frequency ω_0 where the system has three allowed zones separated by two band gaps [26]. The bands are $2\pi/3$ periodic, in agreement with the discussed symmetry property of the Bloch states. Each of the three indicated Chern numbers differs from 0 and their sum gives
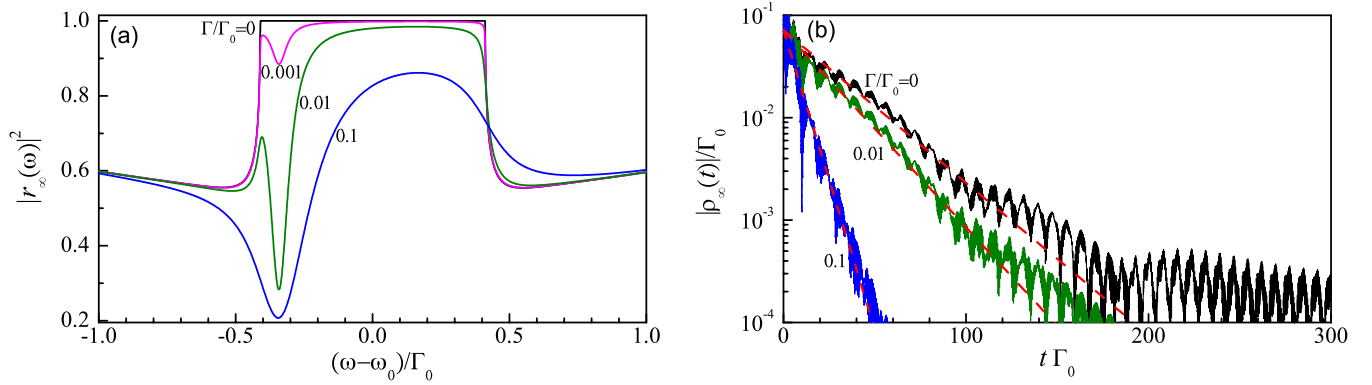
FIG. 3 (color online). (a) The stationary reflection spectra $|r_\infty(\omega)|^2$ for the semi-infinite structure with $\varkappa = \phi - \pi/6 = \pi/2$, $\eta = 0.2/\pi$, $\Gamma_0/\omega_0 = 3 \times 10^{-3}$ and various values of the nonradiative damping Γ. (b) The short pulse response function $\rho(t)$ of the structure. The dashed lines describe the edge mode contribution to the reflection and are plotted after Eq. (9).

zero. As a consequence the structure possesses two edge modes with the energies in the band gaps. The real parts of mode eigenfrequencies are shown by lines in Fig. 2(a), the solid and dashed lines correspond to the mode localized on the left and right edges, respectively. Figure 2(a) demonstrates that the edge modes traverse the band gaps when the parameter $\varkappa$ is varied from $-\pi$ to π. As expected, the inversion symmetry $\varkappa \to -\varkappa$ swaps the left- and right-edge modes. The fact that the edge states for the values $\varkappa$ and $-\varkappa$ are localized at opposite interfaces reflects the "topological protection" of the lattice (n, m).

Since the optical lattice is open the edge eigenmodes are nonstationary. The imaginary part of eigenfrequencies and the edge-mode spatial decay per unit cell, $\mathrm{Im}\{k(\Omega)\}D$, are shown in Figs. 2(b) and Fig. 2(c). The figures demonstrate that the structure has two edge eigenmodes for all values of $\varkappa$ excepting six special points. Particularly, for $\varkappa = 0$ and π both edge states vanish: $\mathrm{Im}\{k(\Omega)\}D \to 0$, $\mathrm{Im}\Omega \to 0$. This occurs because, for these particular values of $\varkappa$, the structure is invariant under the reversal $\varkappa \to -\varkappa$ and hence centrosymmetric. For the other four special points $\varkappa = \pm\pi/6$ and $\pm 7\pi/6$, the spacing between two adjacent resonant layers $\mathcal{A}$ equals to $\lambda_0/2$ and, as a consequence, one of the edge states disappears. For the most values of $\varkappa$ the edge modes are well defined and localized within a few structure periods. Figure 1 shows the spatial distribution of the absolute value of the edge-mode electric field for the five-period structure with $\varkappa = \pi/2$.

Now we focus on the problem of the edge states detection. For example, we consider the semi-infinite structure with $\varkappa = \pi/2$ marked by the star in Fig. 2. For this value of $\varkappa$ the central allowed band shrinks and the values of $\mathrm{Re}(\Omega - \omega_0)$ have opposite signs for the left- and right-edge modes, see Fig. 2. The reflection spectrum $|r_\infty(\omega)|^2$ for the semi-infinite structure is shown in Fig. 3(a). The black curve corresponds to the absence of nonradiative damping. In this case the edge state does not reveal itself in the spectrum. For $\Gamma > 0$ the edge state shows

up as a dip in the reflection spectrum and a peak in the absorption spectrum. Similar approach has been used in Refs. [27,28] to detect conventional Tamm states [29,30] in 2D centrosymmetric photonic crystals. The position and half-width of the reflectivity dip are determined, respectively, by the real and imaginary parts of Ω,

$$\Omega = \omega_0 - \frac{2\Gamma_0 \sin(3\pi\eta/2)}{\sqrt{2 + e^{-3i\pi\eta}}} - i\Gamma. \tag{8}$$

An alternative method of detecting the edge modes is the time-domain optical spectroscopy. The system can be described by the time-resolved reflection response $\rho(t) = \int_{-\infty}^{\infty} r(\omega) \exp(-i\omega t) d\omega/(2\pi)$ induced by the short δ-pulse [31]. Such technique is sensitive both to the amplitude and phase of the reflection coefficient. The edge state should reveal itself as an exponential contribution to the response function given by the residue of $r_\infty(\omega)$ at the frequency Ω,

$$\rho_\Omega(t) = -\Gamma_0 \frac{(1 - e^{3i\pi\eta})^2}{(1 + 2e^{3i\pi\eta})^{3/2}} e^{-i\Omega t}. \tag{9}$$

Thus, the information about the phase missing in $|r(\omega)|^2$ shows up in $\rho(t)$. In Fig. 3(b) the response function $\rho_\infty(t)$ is presented in the semi-logarithmic scale. It indeed contains an exponentially decaying contribution that perfectly agrees with Eq. (9) (see dashed curves). This contribution is already present for $\Gamma = 0$ although the edge state is not revealed in the stationary reflectivity. At longer times the exponential decay of the edge state is masked by the $t^{-3/2}$ power-law contribution of the Bloch-states continuum, the black curve in Fig. 3(b) [31].

To summarize, we have demonstrated the presence of radiative topologically protected edge states in 1D resonant photonic crystals with a compound noncentrosymmetric unit cell. The edge states are shown to survive despite the long-range light-induced coupling of the resonances and

finite lifetime of their radiative decay. The states are manifested in the stationary reflection spectra of the structure with finite nonradiative losses as well as in the time-dependent response to the short optical pulse. The plasmonic lattices with high enough radiative decay rate Γ_0 are preferential for the observation of edge states [19].

---

  [*]poshakinskiy@mail.ioffe.ru

[1] M. Z. Hasan and C. L. Kane, Rev. Mod. Phys. **82,** 3045 (2010).

[2] L.-J. Lang, X. Cai, and S. Chen, Phys. Rev. Lett. **108,** 220401 (2012).

[3] Y. E. Kraus and O. Zilberberg, Phys. Rev. Lett. **109,** 116404 (2012).

[4] Y. E. Kraus, Y. Lahini, Z. Ringel, M. Verbin, and O. Zilberberg, Phys. Rev. Lett. **109,** 106402 (2012).

[5] S. Ganeshan, K. Sun, and S. Das Sarma, Phys. Rev. Lett. **110,** 180403 (2013).

[6] A. Quandt, Physics **5,** 99 (2012).

[7] A. Poddubny and E. Ivchenko, Phys. Solid State **55,** 905 (2013).

[8] S. Ryu, A. P. Schnyder, A. Furusaki, and A. W. W. Ludwig, New J. Phys. **12,** 065010 (2010).

[9] F. D. M. Haldane and S. Raghu, Phys. Rev. Lett. **100,** 013904 (2008).

[10] Z. Wang, Y. D. Chong, J. D. Joannopoulos, and M. Soljačić, Phys. Rev. Lett. **100,** 013905 (2008).

[11] M. Hafezi, E. A. Demler, M. D. Lukin, and J. M. Taylor, Nat. Phys. **7,** 907 (2011).

[12] M. Hafezi, S. Mittal, J. Fan, A. Migdall, and J. M. Taylor, Nat. Photonics **7,** 1001 (2013).

[13] T. Kitagawa, M. A. Broome, A. Fedrizzi, M. S. Rudner, E. Berg, I. Kassal, A. Aspuru-Guzik, E. Demler, and A. G. White, Nat. Commun. **3,** 882 (2012).

[14] M. C. Rechtsman, Y. Plotnik, J. M. Zeuner, D. Song, Z. Chen, A. Szameit, and M. Segev, Phys. Rev. Lett. **111,** 103901 (2013).

[15] M. C. Rechtsman, J. M. Zeuner, Y. Plotnik, Y. Lumer, D. Podolsky, F. Dreisow, S. Nolte, M. Segev, and A. Szameit, Nature (London) **496,** 196 (2013).

[16] A. B. Khanikaev, S. H. Mousavi, W.-K. Tse, M. Kargarian, A. H. MacDonald, and G. Shvets, Nat. Mater. **12,** 233 (2012).

[17] A. Poddubny, A. Miroshnichenko, A. Slobozhanyuk, and Y. Kivshar, ACS Photonics **1,** 101 (2014).

[18] E. L. Ivchenko, *Optical Spectroscopy of Semiconductor Nanostructures* (Alpha Science International, Harrow, England, 2005).

[19] R. Taubert, D. Dregely, T. Stroucken, A. Christ, and H. Giessen, Nat. Commun. **3,** 691 (2012).

[20] T. Weiss, N. A. Gippius, G. Granet, S. G. Tikhodeev, R. Taubert, L. Fu, H. Schweizer, and H. Giessen, *Photonics and Nanostructures—Fundamentals and Applications* 9, 390 (2011).

[21] M. F. Yanik, W. Suh, Z. Wang, and S. Fan, Phys. Rev. Lett. **93,** 233903 (2004).

[22] K. A. Madsen, E. J. Bergholtz, and P. W. Brouwer, Phys. Rev. B **88,** 125118 (2013).

[23] A. N. Poddubny, L. Pilozzi, M. M. Voronov, and E. L. Ivchenko, Phys. Rev. B **80,** 115314 (2009).

[24] S.-Q. Shen, *Topological Insulators. Dirac Equation in Condensed Matters*, Springer Series in solid-state sciences (Springer, Heidelberg, 2013).

[25] A. N. Poddubny and E. L. Ivchenko, Physica (Amsterdam) **42E,** 1871 (2010).

[26] E. L. Ivchenko, M. M. Voronov, M. V. Erementchouk, L. I. Deych, and A. A. Lisyansky, Phys. Rev. B **70,** 195106 (2004).

[27] S. A. Dyakov, A. Baldycheva, T. S. Perova, G. V. Li, E. V. Astrova, N. A. Gippius, and S. G. Tikhodeev, Phys. Rev. B **86,** 115126 (2012).

[28] G. V. Li, E. V. Astrova, S. A. Dyakov, A. Baldycheva, T. S. Perova, S. G. Tikhodeev, and N. A. Gippius, Physica Status solidi (RRL)—Rapid Research Letters 7, 481 (2013).

[29] A. P. Vinogradov, A. V. Dorofeenko, A. M. Merzlikin, and A. A. Lisyansky, Phys. Usp. **53,** 243 (2010).

[30] M. Kaliteevski, I. Iorsh, S. Brand, R. A. Abram, J. M. Chamberlain, A. V. Kavokin, and I. A. Shelykh, Phys. Rev. B **76,** 165415 (2007).

[31] A. V. Poshakinskiy, A. N. Poddubny, and S. A. Tarasenko, Phys. Rev. B **86,** 205304 (2012).